Spatial-Temporal Models for Visual Field Pathology

Raymond G Hoffmann, Edgar A Deyoe, Julie Brefcynski, Manoj Thakur, Daniel B Rowe
The Medical College of Wisconsin
hoffmann@mcw.edu

Abstract

By presenting visual targets around a fixed focus and observing the corresponding activation in the visual cortex with fMRI, an inverse map (retinopic) of the cortex to a circular disk can be obtained. This visual field diagram is potentially a 1-1 map of the visual cortex; however, the structure of the visual cortex means some points will be functional but not anatomic neighbors. When pathology due to disease or trauma is present in the visual cortex, there is reduced or zero response in corresponding areas of the visual map. In addition, if there are changes over time in the extent or magnitude of the pathology (recovery or progression), there should be detectable changes in the visual map. A spatial-temporal approach (discrete time realizations of the spatial process) is used to estimate the spatial mean, variance, and covariance, rather than the more common fMRI temporal-spatial approach (a spatial realization of discrete time series). Simulated lesions of differing extent and magnitude will be used to estimate the sensitivity and specificity of the model to changes in activation or regions not consistent with the surrounding area.

Keywords: fMRI, geostatistics, space-time model,

Introduction

The visual field diagram (VFD) is formed by reverse mapping of areas of the visual cortex to the visual area stimulated by a dense array of visual targets and visual distracters. It is a mapping of the activated voxels of the visual cortex to a circular disk that corresponds to the visual field of the eye. The magnitude of the response is the magnitude of the activation in the cortex. The location is based on the location of the stimulus. If there is damage to the visual cortex, it may be represented by missing or abnormal responses in the induced visual field map. [Brefczynski]

Analytic methods for changes in the VFD, have mainly been ANOVA based [Merriam, 2003]and do not make use of the spatial structure nor do they explore the correlations implicit in the spatial structure. [Hoffmann, 2004]

The Visual Field Diagram

The visual field diagram is formed by an inverse mapping of areas of the visual cortex to the retinopic area stimulated by an array of visual targets. Figure 1 (Brefczynski, 1999) shows the stimuli delivered to the targets, the corresponding areas of the brain that are stimulated and the map that forms the visual field diagram.

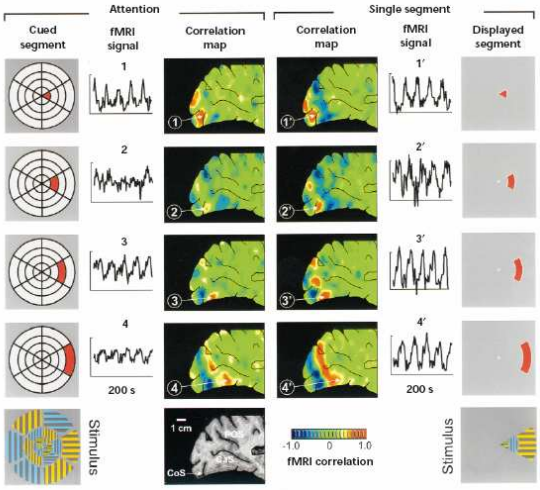

Figure 1 from "A physiological correlate of the 'spotlight' of visual attention" Julie Brefczynski, Edgar DeYoe. Nature Neuroscience 4: 370ff. , 1999

Different stimuli can be used, e.g. a random wedge, a random annulus, a random arc of a web, a wedge that rotates slowly or a wedge that rotates randomly for a shot period of time. This would or could be analogous to an event related design of both the size and shape of the stimuli.

Scientific Research Questions

There are several different types of questions that can be about the visual field: (1) to detect changes in the visual response (VFD) over time or over different stimuli, (2) to detect changes in the response due to healing in stroke, (3) to detect short term or long term changes due to a disease/condition such as migraine or (4) is a blank spot or an area of reduced response in the visual field unusual (tumor, stroke) or within the usual variability?

Brefczynski and DeYoe show that distinct regions in the visual cortex are activated by different targeted tasks. In the case of a normal response, the regions are distinct and non-overlapping nature. of the regions. Right and left visual stimuli induce corresponding non-overlapping right and left regions of the visual cortex.

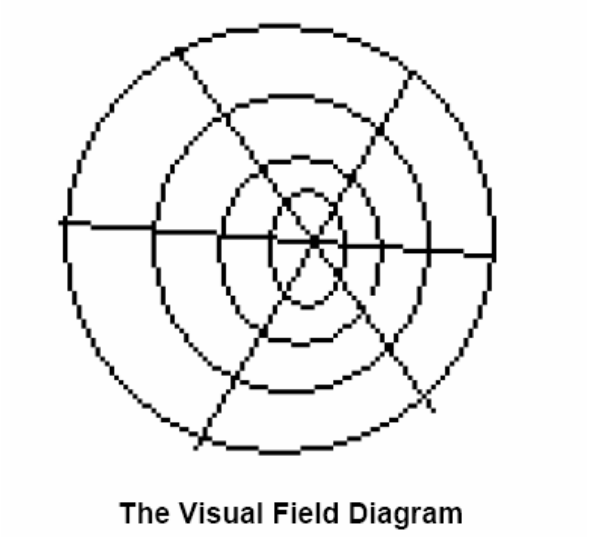

The locations of the points, figure 3, from the inverse map represent the center of a 3D voxel obtained from the fMRI scan. This pattern differs across subjects, so to combine subject information, a geostatistical approach that allows interpolation from the observed points to a common set of points across all subjects is proposed by this study. We will use repeated scans to establish the mean response and the variability in order to be able to determine random changes from significant trends.

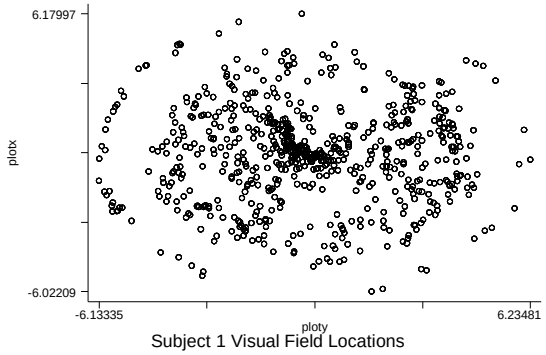

Figure 3. Location of the points for single subject.

An **Areal** approach to the data divides the regions of the visual field map into distinct "areas" or regions.

Figure 4 below shows an areal summary of the magnitude of the activation data from repeated scans on two separate subjects. Clearly there are similarities over time. Since the fMRI scan is not standardized to absolute levels of blood flow, how much of the differences in the figures are due to a need to detrend and center the data over time?

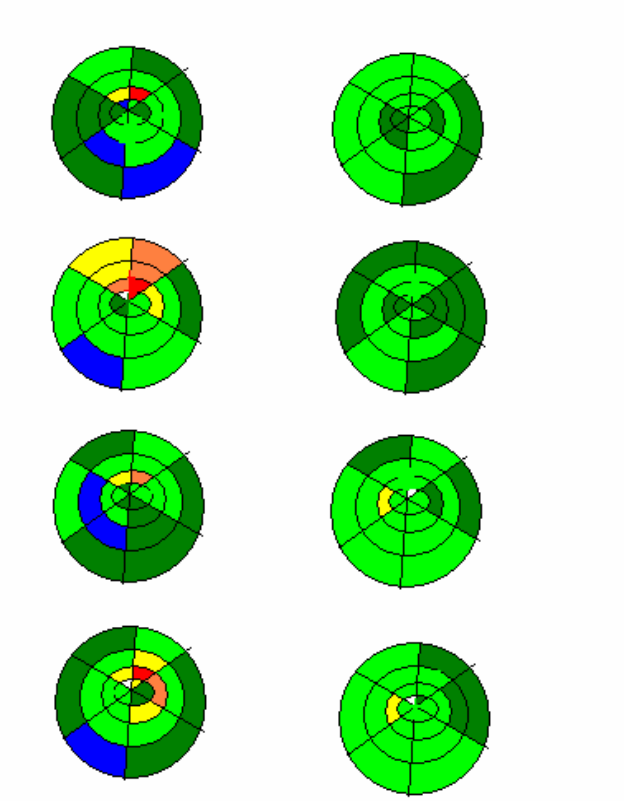

Figure 4: An Areal map of the activation obtained by averaging over the somewhat arbitrarily defined areas of the VFD.

Areal analysis, for the segments can be modeled by a GEE with a general correlation structure.

$$Y_{ijt} = \mu + \nu_i + \alpha_j + \tau_t + \varepsilon_{ijt} \quad \text{and}$$

$$\text{Var}(Y) = I\,\sigma^2 + \Sigma_\rho$$

- where ν_i is the subject effect
- α_j is the segment effect
- τ_t is scan run (time)
- ε_{ijt} is the (correlated) error and
- I is the identity matrix and Σ is the correlation matrix.

This type of statistical model potentially allows considerable flexibility in spatial correlation among the

segments and over time when an unstructured error model is used to estimate the links among the segments. [Hoffmann, 2004].

The Geostatistical Model

The geostatistical approach to spatial data uses each point in the segment. There are 450 to 650 points in a Visual Field. The data is spatially rich and temporally poor. The sample run has five temporal scans. This is quit different form many of the spatial-temporal models that have been based on climate or atmospheric pollutant data (Huerta - Mexican City ozone levels, Carroll – Texas Ozone exposure, Peng – wildfire risk, Hartfield – daily or hourly temperature). For example, Carroll et al have a very long time series of 24 hourly values x 365 days x 14 years at 11 stations. Winkle's study of ocean winds uses remote sensing data to obtain both spatially dense information and temporal data. However, he is able to use a dynamic model for the propagation of the winds from one point to another that is usually not available for most space-time modeling situations. Their goal is often to identify spatial heterogeneity in the seasonal components. Thus considerable complexity is invoked in the temporal modeling.

With only a few repeated scans, the temporal part of an fMRI spatial-temporal model will be substantially simpler in this application. However, the ability to assess differences in the spatial pattern over time (scan) is the one of the key goals. The innate correlation of the regions of the visual field makes it necessary to consider a spatial correlation model together with a (simple) model of the correlation over scan. Clearly, this correlation is the correlation of the residuals after the trends due to experimental stimulations have been removed.

However, this model has short time series corresponding to only a few tasks or conditions per session – for example, Brefzinski is using 5 per session. Multiple sessions can conceptually be used either to test for the effect of an innovation such as a migrane headache or for changes in the visual field due to stroke recovery. Because the time courses are usually short, we will use fairly simple models for temporal modeling for the residuals. A simple autocorrelation model – AR(1) or AR(2) is conceptually the limit longitudinally diring the session. Since fMRI can show a drift over time, we use a discrete model $\mu_i(t) = \mu_{it}$ which essentially models the average baseline shift of each baseline. This differs from climatologic models which usually have very long time series so they can model the spatial variability of similar time series.

We can only do the second in the following model:

$$Z(s,t) = \mu_\alpha(s,t) + g_\beta\{Y(s),t\} + W_\xi(s,t) + \varepsilon_\sigma(s,t)$$

where Z(space,time) is composed of
$\mu_\alpha(s,t)$ is the spatial trend
$g_\beta\{Y(s),t\}$ is the temporal process
which may also vary spatially
$W_\xi(s,t)$ is the spatial temporal error process
with 0 mean
$\varepsilon_\sigma(s,t)$ is the random field with 0 mean

The spatial trend $\mu_\alpha(s,t)$ can be modeled as a low order polynomial or estimated non-parametrically with a 2D smoother – kriging. There are many choices for the type of kriging: simple, block, ordinary, universal, etc. The spatial-temporal trend $g_\beta\{Y(s),t\}$ will include the innovation terms that appear from task to task or from session to session as well as the global spatial normalization terms $\gamma_i(t)$ from scan to scan or session to session. For repeated scans within a single session, we will use a discrete model $\gamma_i(t) = \gamma_{it}$ which essentially models the average baseline shift or drift over time. For scans over multiple sessions, we'll use a random effects model for the session.

The error processes $W_\xi(s,t) + \varepsilon_\sigma(s,t)$ will usually be broken into several components. We will assume initially that $W_\xi(s,t)$ can be <u>separated</u> into a spatial process and a temporal process. Because the time courses are usually short, we will use fairly simple models for the temporal modeling of the residuals. A simple autocorrelation model – AR(1) or AR(2) is conceptually the limit longitudinally during the session. By estimating the AR(1) parameters separately for each location and smoothing the result, the spatial homogeneity of the temporal process can be determined.

Example

The pattern is not the same for each subject. Although there appear to be gaps in the Visual Field Diagram, these do not correspond to blind spots or damage to the retina of these control subjects. They are instead due to the discrete voxelated nature of the information about the activation of the visual cortex obtained from fMRI. Figure 5 shows the differences in the location

of the points across subjects. Clearly interpolation of the location data is needed.

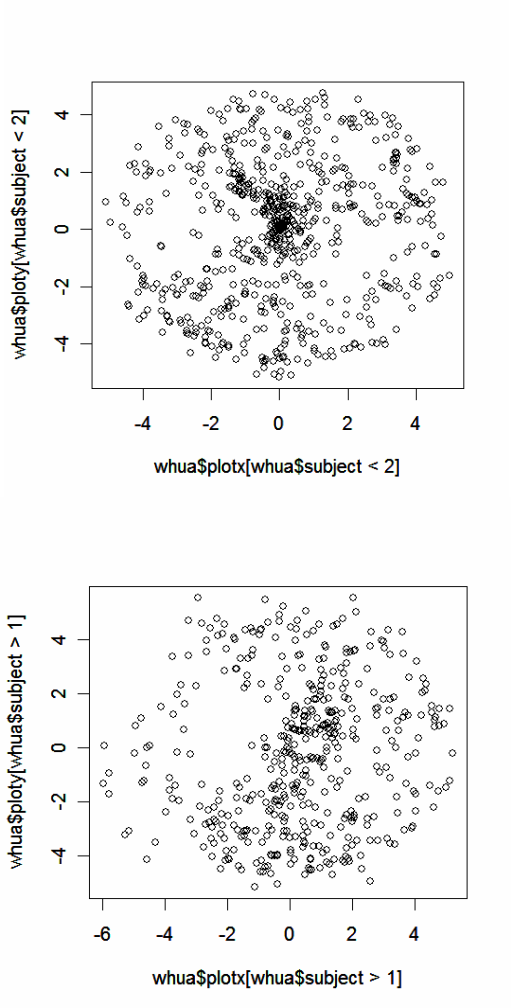

Figure 5. Differences in the location of the activation points across subjects.

Kriging is the geostatistical term for a class of methods for predicting the values between the observed points which is critical in terms of being able to combine results across subjects. [Bailey, Cressie]

Simple kriging assumes that the first order component μ(s) is known a priori and does not have to be estimated from the data. Then the values for the process a unobserved points can be determined from the known spatial trend and a linear combination of the observed residuals using weighted least squares. The weights depend on the known spatial covariance structure.

In practice, we need to estimate both the trend surface and the spatial covariance structure. Ordinary kriging extends this process to estimating the trend and covariances under the assumption that the spatial trend is a constant independent of location. Universal kriging takes the process a step further to the assumption that we are estimating a trend X(s)β from the data and the covariances; however, universal kriging implicitly estimates this surface by generalized least squares and, thus, does not allow testing of whether a specified model fits the data. An alternative strategy if the focus is on estimation of the spatial process is block kriging which estimates the covariances in a local neighborhood of the data so that the spatial trend can be ignored. For this method to work, a dense set of observed spatial data is needed. Consequently, it is not very useful in the ozone climatology model and while there are enough points in the usual VFD map, the gaps in the points suggest that it is not a good choice for fMRI data either. Since the innovation in fMRI will usually be known, an good alternative to kriging is to estimate the trend surface by general least squares and then use the residuals to examine the spatial process.

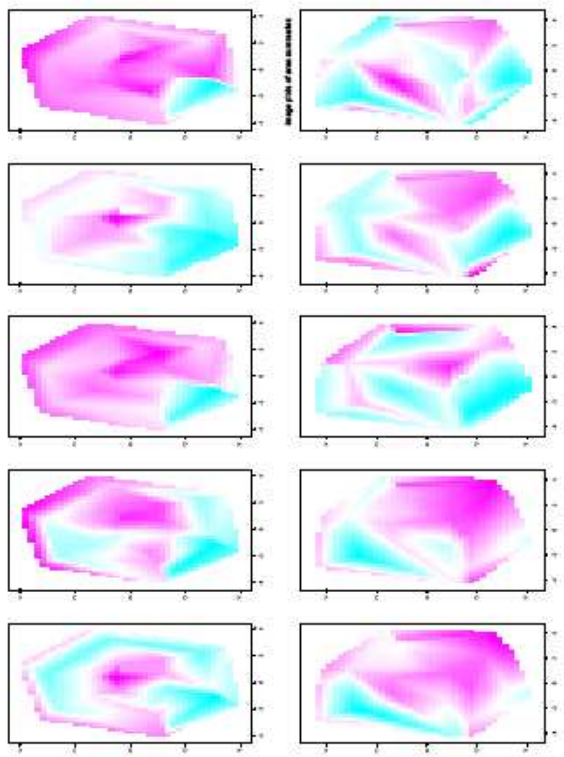

Figure 6. Slightly smoothed replications using Splus/R

The data that will be used to estimate the parameters of the model under spatial and temporal homogeneity are based on 5 repeated scans in each of two subjects. A

smoothed version of the data is displayed in figure 6. Similarities in the global pattern, the trend surface, can be seen both over time within a subject and across subjects. The 2 subjects with the 5 replicates without an intervention allow estimation of the spatial and temporal autocorrelation.

Spatial Analysis Software Available in R

The libraries in R are continually bein added to and developed. There are many R libraries that are primarily associated with spatial point data, such as spatial, spatstat, splancs, etc. An overview of some of these libraries can be found in Ripley.

R libraries that are particularly useful for geostatistical data analysis are:

spatial (part of MASS) – the library spatial, documented in Venebles and Ripley, is particularly useful for determining trend surfaces: polynomial trend surfaces, lowess trend surfaces and kriging.

gstat – the library gstat [Pebesma] is designed for multivariate geostatistical modeling. It provides simple kriging, block kriging, cokriging (kriging with multiple variates making up the surface). It will compute variograms and cross-variograms, even when the multivariable data are not measured at the same points. In addition, it will simulate spatial data from a Gaussian random field with a given variogram

geoR – The library geoR implements methods for Gaussian (and transformed Gaussian) models. In addition to methods for exploratory analysis geoR implements simple, ordinary, universal and external trend kriging. It implements conditional simulation and simulations for Bayesian inference when predicting a a specified location. [Ribeiro]

geoRglm – The library geoRglm is an extension of geoR to linear spatial models using MCMC (Markov Chain Monte Carlo) methods to implement conditional simulation for the Poisson and Binomial generalized linear models.

sgeostat – The modeling tools in sgeostat are chiefly concerned with the prediction, with known confidence, of a spatial stochastic process, {$\boldsymbol{Z}(\boldsymbol{s})$: $\boldsymbol{s}$ (is in) D}, at an arbitrary location, $\boldsymbol{s}0$, from data, {z($\boldsymbol{s}$1),...,z($\boldsymbol{s}$n)} by characterizing the spatial dependence of the process from the data and using a model of the dependence to construct a predictor that minimizes the mean squared prediction error. The spatial dependence is characterized through the variogram. The empirical variogram is used in exploratory analysis, parametric variogram model fitting, and spatial prediction. The exploratory techniques include many of those described in section 2.2 of Cressie (1993), including lagged scatter plots, variogram cloud scatter plots and variogram cloud box plots.

Estimation of Spatial Trend

Exploring the trend surface using both polynomial assumptions and kriging allows evaluation of some of the different techniques available in R. Using the R library **spatial** we can test the effect of the order polynomial on the estimated trend surface

Comparison of the fifth order polynomial over time and across subjects can be observed in the following figure 7. The R code to create the surface, set the plot boundaries and perform a contour plot of the data is for a second order polynomial is

```
j11.2 <-surf.ls(2,j11$plotx,j11$ploty,j11$LC0)
trs11.2 <-trmat(j11.2,0, 6.5, 0, 6.5, 30)
contour(trs11.2)
title("order 2 polynomial trend")
```

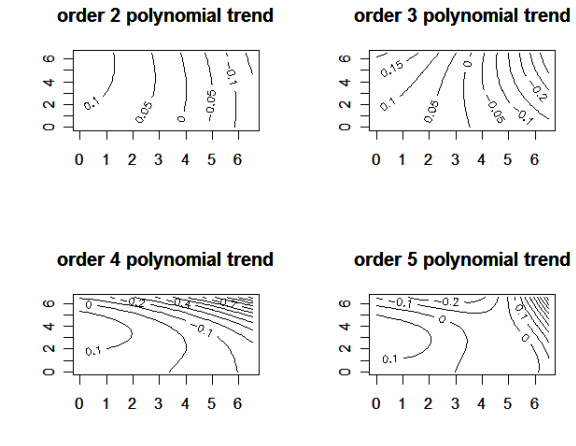

Figure 7: Different order polynomial trends.

Comparisons of the polynomial trend surfaces for two different scans and for the two subjects are displayed in figure 8. The similarity of the fifth order polynomials shows its effectiveness at modeling the trend surface over replicates of the scans with no innovations. Potentially the fifth order polynomial is also including some of the noise process because of the differences in the fine detail over time.

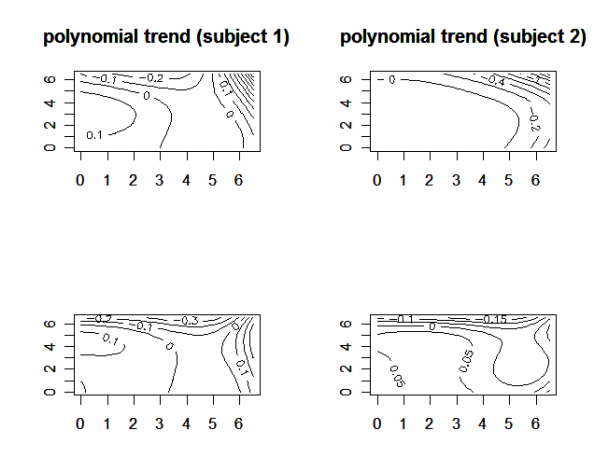

Figure 8. Polynomial trend surfaces at different scans and for the two subjects

Figures 7 and 8 do not take the spatial structure into account. Using general least squares with an estimated correlation model or using universal or block kriging allows models that incorporate this aspect of the VFD.

Estimation of Spatial Correlation

The variogram allows estimation of the spatial correlation by examining all pairwise comparisons of the points. Using the R library spatial, we can easily create the variograms for scan replicates for each of the sample VFD's in figure 9.

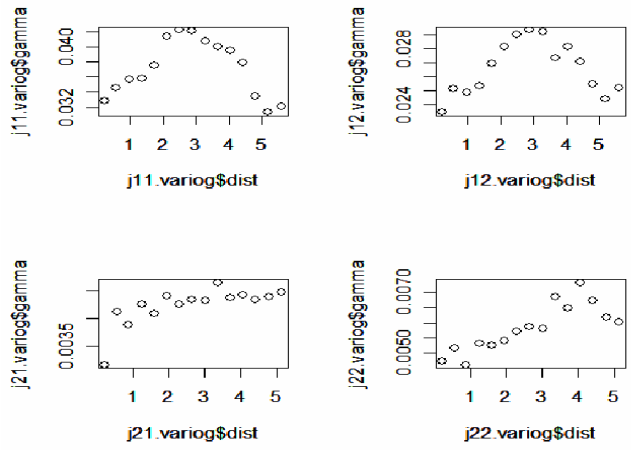

Figure 9. Variogram estimates within and across subjects.

Of course, since the data is spatial, the correlation may depend on the direction that it is examined. A VFD that has the same spatial correlation in each direction is said to be isotropic. Clearly this is desirable from a modeling point of view. Isotropy can be examined with the directional variogram which partitions the correlation estimation into different directions. Traditionally this is done in terms of the 4 angles 0, 45, 90 and 135 degrees. The library gstat will do this automatically and the result for subject 1 - scan 1 is displayed in figure 10.

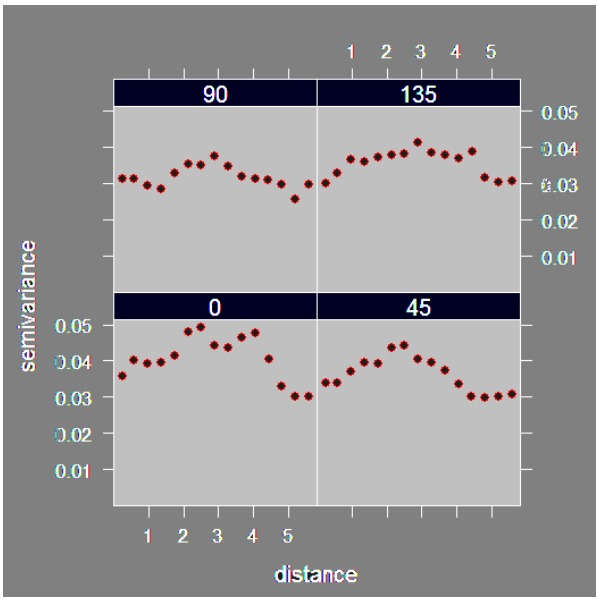

Figure 10. Directional Variogram for a single subject and a single scan.

If the variograms were different, the spatial process would be termed anisotropic. However the similarities are quite evident.

Combined Estimation of Spatial Trend and Spatial Correlation

Using generalized least squares or universal kriging we can combine the estimation of the spatial trend and the estimation of the spatial correlation. The results of this using the R library spatial is displayed in figure 11.

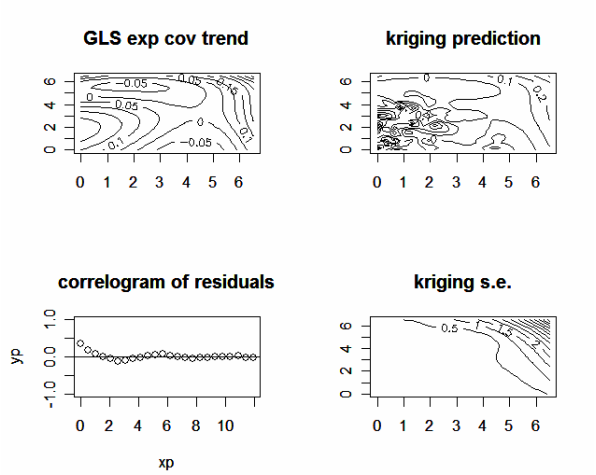

Figure 11. General least squares prediction and correlation on the residuals are displayed on the right side of the figure. The surface and the standard effort of the surface from a fifth degree universal kriging is displayed on the left side of the figure.

Future Directions

Use a known innovation on top of a known spatial trend with a variogram similar that estimated from this example data to test the ability to identify spatial temporal changes due to innovations as well as differences in the spatial structure. Identify outliers or unexpected changes in the trend surface using either robust kriging or using the residuals from the global spatial temporal fit.

References

Bailey T and Gatrell A. Interactive Spatial Data Analysis. Prentice Hall. 1995

Banerjee S, Gelfand SB and Carlin BP. Hierarchical Modleling and Analysis for Spatial Data. CRC Press, 2003 – using WinBugs

Brefczynski J, DeYoe EA. "A physiological correlate of the 'spotlight' of visual attention". Nature Neuroscience 4: 370ff. , 1999.

Carroll RJ, Chen R, George EI, Li TH, Newton J, Schmiediche H and Wang N. "Ozone Exposure and Population Density in Harris County, Texas." JASA. 92:392-416. 1997.

Chandler R, Isham V and Northrop P. "Spatiotemporal Rainfall Processes: Stochastic Models and Data Analysis". Statistical Computing and Graphics Newsletter, V. 8, #2/3 (ASA CG web site)

Cressie N. Statistics for Spatial Data. Revised. 1993. John Wiley and Sons. New York.

Elliott P, Wakefield J, Best N and Briggs D. Spatial Epidemiology. Oxford. 2000

Griffith DA and Layne L. A Casebook of Statistical Data Analysis: A Compilation of Analyses of Different Thematic Data Sets. Oxford University Press. 1999.

Hartfield ML and Gunst RF. "Identification of model components for a class of continuous spatiotemporal models. JABES. 2003.

Hoffmann RG. "Techniques for fMRI Visual Field Diagram Analysis". Proceedings of the American Statistical Association, 2004.

Huerta G and Sanso B. "A spatio-temporal model for Mexico City ozone levels". Applied Statistics. 53(2):231-248. 2004.

Merriam EP, Genovese CR, Colby CL. Spatial Updating in the Human Parietal Cortex. Neuron. 39:361-373, 2003.

Pebesma EJ. "Gstat: multivariable geostatistics for S". in DSC 2003 Working Papers. http://www.ci.tuwein.ac.at/Conferences/DSC-2003

Peng RD, Dominici F, Pastor-Barriuso R, Zeger SL, and Samet JM. "Seasonal Analyses of Air Polution and mortality in 100 US cities." Am. J Epidem. 2005. 161:585-594.

Peng RD, Schoenberg FP, Woods JA. "Space time conditional intensity model for wildfire hazard" JASA. 2005. 100:26-35.

Raghavan N and Goel PK. Modeling and Characterizing Microstructures Using Spatial Point Processes. Statistical Computing and Graphics Newsletter, V. 8, #2/3 (ASA CG web site).

Ribeiro PJ, Christensen OF and Diggle PJ. "Geostatistical software – geoR and geoRglm". In DSC 2003 Working Papers. http://www.ci.tuwein.ac.at/Conferences/DSC-2003.

Ripley B. "Spatial statistics in R". R news. Vol. 1/2:14-15.

Venables W and Ripley B. Modern Applied Statistics with S. Chapter 15. (4th ed.). Springer-Verlaag. 2002. – using SPlus and R

Winkle CK, Millif RF, Nychka D and Berliner LM. "Spatiatemporal hierarchical Bayesian modeling: tropical ocean surface winds". JASA. 2001. 96:382-397.